GaN BUFFER DESIGN: ELECTRICAL CHARACTERIZATION AND PREDICTION OF THE EFFECT OF DEEP LEVEL CENTERS IN GaN/AlGaN HEMTs

M. Silvestri[a], M. J. Uren[a], D. Marcon[b], and M. Kuball[a]

[a] Center for Device Thermography and Reliability (CDTR), H.H. Wills Physics Laboratory, University of Bristol, Tyndall Avenue, Bristol BS8 1TL, UK
[b] IMEC, Kapeldreef, 75. B-3011, Leuven, Belgium

[*] E-mail: marco.silvestri@bristol.ac.uk, Phone: +44 117 928 8734, Fax: +44 117 925 5624

Abstract

GaN buffer deep level centers are studied coupling measurements and device physics simulations. The impact of Fe- and C-doped samples on low frequency device transconductance and noise is presented. The Fe-level found at 0.7 eV below the GaN conduction band results in low frequency generation-recombination noise and transconductance dispersion. The agreement with the model shows that the buffer can now be reliably simulated and used to investigate the impact of other deep level traps, such as carbon, that cannot be easily measured due to their deep position in the GaN bandgap.

I. Introduction

The quality of GaN material and GaN-based high Electron Mobility Transistor (HEMT) technology has increased remarkably during the last few years. A significant number of markets such as automotive, satellite communications, and high-power signal management are heavily investing in the development of GaN technology due to the promising delivered performance [1]. To achieve such results though, detailed understanding of all the limiting issues that still pose restrictions on this technology must be gained.

Although the engineering of the gate shape has strongly reduced current collapse [2], the impact of deep centers on the device switching performance is not fully understood and modeled. Furthermore, the use of deep levels to suppress short channel effects in GaN HEMTs, reducing the conductivity of the grown GaN buffers, is essential [3]. Relying on intrinsic growth defect centers is a widely used solution, but the capability to control extrinsic defects during growth and achieve a finely controlled insulated buffer is becoming more attractive and a more detailed understanding of the deep levels of GaN is fundamental.

Iron and carbon are the most commonly used impurities. They lead to two different deep acceptor centers, one in the upper and one in the lower half of the GaN band gap, respectively, contributing to a different extent to current collapse [4].

In this work, we take advantage of the dynamic transconductance technique, low frequency noise measurements, and ATLAS device simulations on iron and carbon doped AlGaN/GaN HEMTs. The presented approach enables one to predict the behavior of buffer traps and their influence on small signal device performance.

II. Devices and setup

Fe-doped AlGaN/GaN HEMTs grown by metalorganic vapor phase epitaxy (MOVPE) on SiC substrates with 4 µm source-drain gap, 0.25 µm channel length, and 26 nm AlGaN layer thickness were studied. Intentional iron doping of the GaN buffer was implemented during growth with three different residual channel concentrations: low ~$7x10^{15}$ cm^{-3}, medium ~$3.6x10^{16}$ cm^{-3}, and high ~$1.5x10^{17}$ cm^{-3} [7].

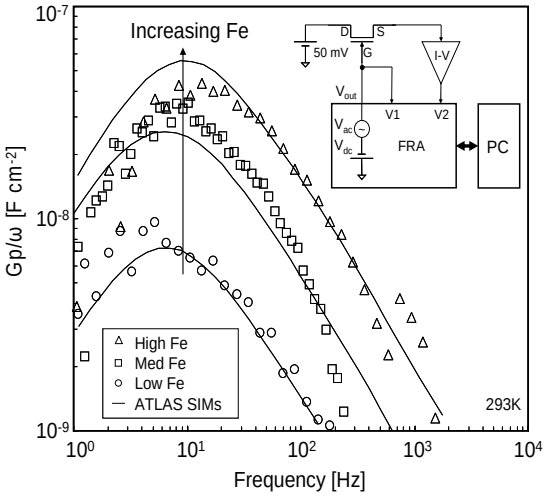

Figure 1: Measured (symbols) and simulated (solid lines) trap conductance vs. frequency at 293 K for three representative 0.25 µm AlGaN/GaN HEMTs with different iron doping concentrations. In the inset the experimental setup is reported.

7 b

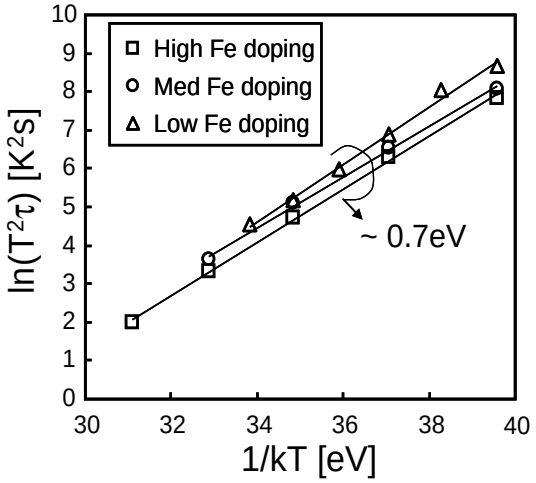

Figure 2: Activation energy extraction in the three iron-doped wafers. All the samples show consistent activation energy around 0.7 eV.

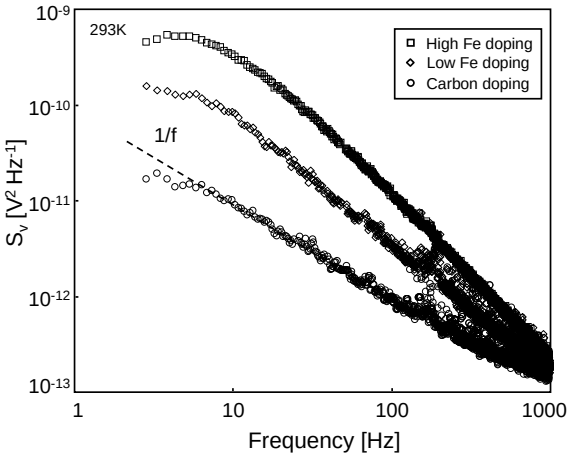

Figure 3: Low frequency noise spectra in iron- and carbon-doped AlGaN/GaN HEMTs at room temperature. Carbon-doped devices show only 1/f behaviour while a G-R peak appears in iron-doped ones.

C-doped 0.5-µm gate length devices with 22-nm thick AlGaN layer on top of 150 nm of undoped and 500 nm of ~$2x10^{17}cm^{-3}$ C-doped GaN layers were also studied.

The devices were measured in the ohmic regime, with a drain bias of 50 mV and the drain current measured with a low noise current to voltage converter over different base plate temperatures. The dynamic transconductance dispersion measurement was performed with a frequency response analyzer in the range 1 Hz–10 kHz (see inset of Fig. 1). More details on the technique can be found in [5] and [6]. Low frequency noise was measured in the 1 Hz–1 kHz range with a fast signal acquisition board.

Simulations were performed with the Silvaco ATLAS code using the approach described in [4] and [6]. The buffer deep level doping was varied in accordance with the measured devices, and a low density (10^{15} cm^{-3}) of shallow compensating donors was included in all cases to model unintentional buffer contamination with species like Silicon.

II. Results and discussion

Fig. 1 reports the measured trap conductance extracted from the dynamic transconductance measurements as a function of frequency at 293 K for three representative 0.25-µm gate length AlGaN/GaN HEMTs with different iron doping concentrations in the buffer. The higher the iron concentration the higher the trap conductance. No conductance bias dependence was observed in all the tested samples confirming the bulk trap nature of the dispersion [8].

Fig 2 shows the extraction of the activation energy from the shift of the extracted conductance peak (i.e., trap characteristic time τ) with temperature. The extraction from the three different wafers was consistent around 0.7 eV with a capture cross section in the 10^{-13}-10^{-14} cm^2 range at 293 K. These values were used as input for ATLAS simulations together with the iron doping distributions in the devices obtained from secondary ion mass spectroscopy (SIMS) analysis described in Ref. [7]. No other fitting parameters were used in the simulations. From the simulated frequency analysis all the transistor Y-parameters were extracted and used to calculate the trap conductance according to [5]. As shown in Fig. 1, the simulations captured very well the experimental behavior. Once the activation energy, capture cross section, and trap concentration are known it is possible to model the behavior of the traps, complementing and guiding the experimental detection as well as predicting, with good accuracy, the effect on small signal performance, as shown in Fig. 1.

In contrast to the Fe-doped devices, C-doped ones did not show any measurable dispersion up to 80 °C. This is because the Fermi level sits near the C-level that has been reported around 0.9 eV above the GaN valence band [9] with a predicted frequency response in the mHz range that is outside our measurement window.

In order to gain complementary insight into the C-trap level, low frequency noise measurements, depicted in Fig. 3, were performed. Fe-doped samples display a distinct generation-recombination (G-R) centre around 10 Hz due to active traps where the Fermi level crosses the Fe level and the G-R mechanism is efficient as sketched in fig. 4b. This is in agreement with the transconductance peak frequency shown in Fig. 1 illustrating that both techniques can be used in parallel to probe traps below the gated portion of the channel where the Fermi level is modulated by the gate as

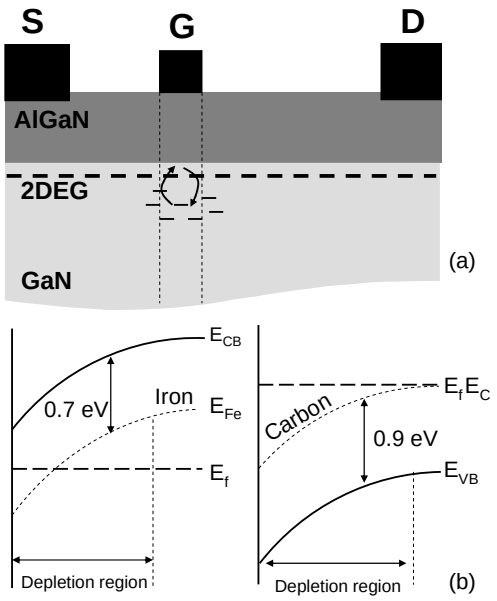

Figure 4: Schematic representation of an AlGaN/GaN HEMT and the region probed by our measurements below the gated portion of the channel (a); Iron and Carbon trap levels: 0.7eV below the conduction band and 0.9eV above the valence band, respectively.

schematically shown in Fig. 4a; the noise peak scales in magnitude with the iron doping concentration as expected. In contrast, the C-doped devices show only 1/f noise behavior, mostly originating in the contact and access region, because the Fermi level is pinned at the C-level, well below the mid gap.

IV. Conclusions

In conclusion we demonstrated through coupled experiments and simulations that the Fe deep-acceptor center with a concentration above 10^{16} cm^{-3} can be electrically characterized through quasi-static electrical techniques due to its position in the upper part of the GaN band gap. Device simulations give remarkably accurate predictions of the observed dispersion behavior confirming the physics implementation, and demonstrating its usefulness for studying the device impact of trap levels that cannot be directly probed. This approach can be generalized to different semiconductor devices being technology independent.

Acknowledgements

The authors would like to thank the UK-EPSRC through grant EP/I033165/1; IMEC, QinetiQ Ltd and the UK MoD for providing the devices.

References

[1] U. K. Mishra et al., *Proc. of the IEEE*, vol. 96, no. 2, 2008
[2] W. Saito et al., *IEEE Trans. Electron Dev.*, vol. 31, pp. 659-661, 2010.
[3] M. J. Uren et al., *IEEE Trans. Electron Dev.*, vol. 53, pp. 395-398, 2006.
[4] M. J. Uren et al., *IEEE Trans. Electron Dev.* , vol. 59, pp. 3327-3333, 2012.
[5] H. Haddara and G. Ghibaudo, *Solid-State Electronics*, vol. 31, no. 6, pp. 1077-1082, 1988.
[6] M. Silvestri, et al., *IEEE Electron Dev. Lett.*, vol. 33, no. 11, pp. 1550-1552, 2012.
[7] M. J. Uren et al., *Proc. 1st European Microwave Integrated Circuits Conference*, pp. 65-68, September 2006.
[8] E. H. Nicollian and J. R. Brews, *MOS physics and technology*, Wiley, New York, 1982
[9] J. L. Lyons et al., *Applied Physics Letters*, vol. 97, 2010.

7
b